AJNR

Tanycytomas: A Newly Characterized Hypothalamic-Suprasellar and Ventricular Tumor

K.A. Lieberman, J.J. Wasenko, R. Schelper, A. Swarnkar, J.K. Chang and G.S. Rodziewicz

AJNR Am J Neuroradiol 2003, 24 (10) 1999-2004
http://www.ajnr.org/content/24/10/1999

AJNR Am J Neuroradiol 24:1999–2004, November/December 2003

Case Report

Tanycytomas: A Newly Characterized Hypothalamic-Suprasellar and Ventricular Tumor

K.A. Lieberman, J.J. Wasenko, R. Schelper, A. Swarnkar, J.K. Chang, and G.S. Rodziewicz

Summary: We report five cases of tumors occurring in three children and in two adults. The tumors had unusual histomorphology and a mixture of ependymal and piloid-like astrocytic features and a myxoid stroma similar to myxopapillary ependymomas. MR imaging in three of the cases showed aggressive, intensely enhancing partially cystic hypothalamic-suprasellar masses near midline and near the floor of the third ventricle. In the three pediatric cases, the tumor encased the circle of Willis. This newly characterized tumor, the tanycytoma, has neoplastic cells with histomorphologic and ultrastructural characteristics similar to those of the tanycyte.

Tihan et al (1), in 1999, described a series of neoplasms occurring in the pediatric population having a distinctive monomorphous pilomyxoid histologic pattern. Most of these tumors were located in the hypothalamic-chiasmatic-suprasellar region. Although these lesions were histologically similar to pilocytic astrocytomas, they had a higher rate of recurrence and dissemination than did the classic pilocytic astrocytoma. A newly characterized tumor composed of cells resembling tanycytes has recently been described in the pathology literature (2). Tanycytes are process-bearing radial glia that persist in mammals and are commonly in the walls of the ventricles of the brain. Tanycyte is derived from the Greek word *tanuz*, meaning a cell that is stretched out (3). The tanycyte processes make contact with capillaries in the brain parenchyma and pial surface, suggesting that they might be involved in the uptake or delivery mechanisms between CSF, blood cells, and hypothalamic cells (4). Our cases are unique in relation to the cases reported by Tihan et al in that they include both pediatric and adult cases and further ultrastructural evaluation by electron microscopy. This current report serves to expand our clinicopathologic experience with the "tanycytoma," with particular attention to the differential diagnosis, imaging, and histiologic characteristics.

Received February 22, 2003; accepted after revision March 20.

From the Departments of Neuroradiology (K.A.L., J.J.W., A.S., J.K.C.), Neuropathology (S.R.), and Neurosurgery (G.S.R.), State University of New York Upstate Medical University, Syracuse, New York.

Address reprint requests to Kristin A. Lieberman, MD, Marshfield Clinic, Department of Radiology, 1000 North Oak Ave, Marshfield, WI 54449.

Case Reports

Five patients (three children and two adults) presented with symptoms similar to those of other hypothalamic-suprasellar neoplasms: headache, nausea, vomiting, and endocrinologic problems. The neoplasms in the children were located in the hypothalamic-suprasellar region and were aggressive tumors. The tumors in the adults, one located in the hypothalamus and the other in the left lateral ventricle, were less aggressive. These patients were able to undergo complete tumor resection and had experienced no recurrence at the time of this writing. The multiplanar compatibilities of MR imaging showed the full extent of the pediatric tumors with hypothalamic to suprasellar extension and encasement of the arteries at the base of the brain. The neoplasms were hypointense on T1-weighted and hyperintense on T2-weighted images relative to the brain parenchyma. After the administration of contrast material, the four neoplasms located in the hypothalamic-suprasellar regions showed intense enhancement. The fifth patient, an adult with a small tumor located in the left lateral ventricle, had slightly hyperintense signal on T2-weighted and fluid-attenuated inversion recovery images relative to brain parenchyma. After the administration of contrast material, minimal enhancement of the tumor was seen. All patients underwent MR imaging of the entire neuroaxis, which did not reveal any additional lesions. The histopathology of the tumors showed a monotonous population of cells with delicate piloid-like processes, loosely arranged within a prominent myxoid background (Tables 1 and 2).

Discussion

These hypothalamic-suprasellar and lateral ventricle tumors had an unusual histopathology with a blend of piloid-like astrocyte and ependymal features and a variable myxoid stroma. The differential diagnosis of a suprasellar-hypothalamic mass includes optic-hypothalamic astrocytoma, craniopharyngioma, germinoma, arachnoid cyst, epidermoid, and dermoid. Pilocytic astrocytoma and myxopapillary ependymoma should be considered in the differential diagnosis for these tumors and histopathologically appear the most similar to our cases. Ependymomas represent 2% to 6% of all intracranial neoplasms. Only a small percentage of these occur in the third ventricle, usually arising from the posterior portion of the third ventricle. Myxopapillary ependymomas appear to occur almost exclusively in the filum terminale and the conus medullaris. To our knowledge, there are no known reported third ventricle myxopapillary ependymomas.

Pilocytic astrocytomas, on the other hand, are common in the hypothalamic-suprasellar region. Optic pathway tumors are commonly of low grade and considered to be of the pilocytic astrocytoma type. This tumor has its highest incidence in children and generally has an indolent biologic behavior. These tumors are associated with a higher incidence in chil-

TABLE 1: Demographic, clinical, and imaging data

Patient No.	Age (y)/Sex	Symptoms	Location	Imaging
1	2/F	Headache, nausea, emesis	Hypothalamus-suprasellar mass	Large, partially cystic intensely enhancing mass; encases circle of Willis
2	2/M	Diplopia, decrease in left eye vision	Hypothalamus-suprasellar mass	Large, intensely enhancing mass; encases circle of Willis; (Fig 2A–D)
3	3/M	Headache, emesis	Hypothalamus-suprasellar mass	Large, partially cystic intensely enhancing mass; encases circle of Willis
4	26/F	Galactorrhea, hypothyroidism	Hypothalamus	Homogeneous enhancing mass (Fig 3A–C)
5	56/F	Headache	Left lateral ventricle	Minimally enhancing, well-defined mass

Note.—F indicates female; M, male.

TABLE 2: Surgical, pathologic, and therapeutic data

Patient No.	Surgery	Therapy	Pathology	Follow-up
1	Partial resection	Radiation: 5012 cGy chemo: carboplatin vincristine	Tanycytes; occlusion of bilateral internal carotid arteries (Fig. 1A–D)	Deceased <1 yr from initial diagnosis; bilateral, massive strokes
2	Partial resection	Radiation: 5040 cGy chemo: carboplatin vincristine	Tanycytes; (Fig. 2E–G)	Decrease residual tumor
3	Partial resection	Radiation: 5400 cGy chemo: carboplatin vincristine	Tanycytes; encased circle of Willis	Deceased <1 yr from initial diagnosis; cardiac arrest
4	Complete resection	Radiation: 5400 cGy	Tanycytes; + GFAP stain, + synaptophysin stain (Fig. 3D and E)	Lost to follow-up
5	Complete resection	None	Tanycytes	No recurrence at 4 months

Note.—Chemo indicates chemotherapy; GFAP, glial fibrillary acidic protein.

dren with neurofibromatosis type 1. Unlike the classic pilocytic astrocytoma, our tumors occurred in pediatric and adult patients and in the pediatric cases, were very aggressive neoplasms leading to less favorable outcomes. In our pediatric cases, the tumors were only partially resectable and continued to grow despite adjuvant treatment with radiation and chemotherapy. One pediatric patient died as a result of bilateral cerebral hemisphere infarctions caused by tumor encasement of the circle of Willis (Fig 1). On the other hand, similar to the pilocytic astrocytomas, no neuroaxis dissemination occurred.

The multiplanar capabilities of MR imaging showed the full extent of these tumors with hypothalamic to suprasellar extension. In the pediatric cases, the neoplasms also extended beneath the frontal lobes and obstructed the third ventricle, resulting in hydrocephalus. The pediatric tumors also encased the circle of Willis leading to unresectability (Fig 2). Similar to pilocytic astrocytomas, these tumors were hypointense on T1-weighted images and hyperintense on T2-weighted images, with solid and cystic components present. Optic-hypothalamic astrocytomas are usually solid masses that are isointense on T1-weighted and hyperintense on T2-weighted images. A cystic component may be present in large masses. Slightly less common than in the classic pilocytic astrocytomas, these newly characterized tumors had intense enhancement of the tumor mass (Fig 2). Mild to moderate enhancement is seen with IV administered contrast material in approximately 50% of lesions. Ependymomas, on the other hand, can be homogeneous or heterogeneous on MR images. Ependymomas usually are slightly hypointense on T1-weighted images and isointense on T2-weighted images. These tumors commonly have cystic components, insinuate into spaces, and encase vessels similar to our cases. Ependymomas may contain foci of calcification, which will differentiate this tumor from pilocytic astrocytomas and this newly characterized tumor.

Craniopharyngiomas consist of the adamantinomatous and papillary types. The adamantinomatous type consists of solid and cystic components similar to our cases but the cystic component is hyperintense on T1- and T2-weighted images. Calcification is also present in approximately 90% of lesions. Moderate enhancement is seen in the solid component with the IV administration of contrast material. Similar to our pediatric tumors, vascular encasement is often present, allowing only partial resection. The papillary type is typically a solid or solid-cystic mass with solid component showing intense enhancement. Germinomas, unlike the lesions in our cases, are hypointense

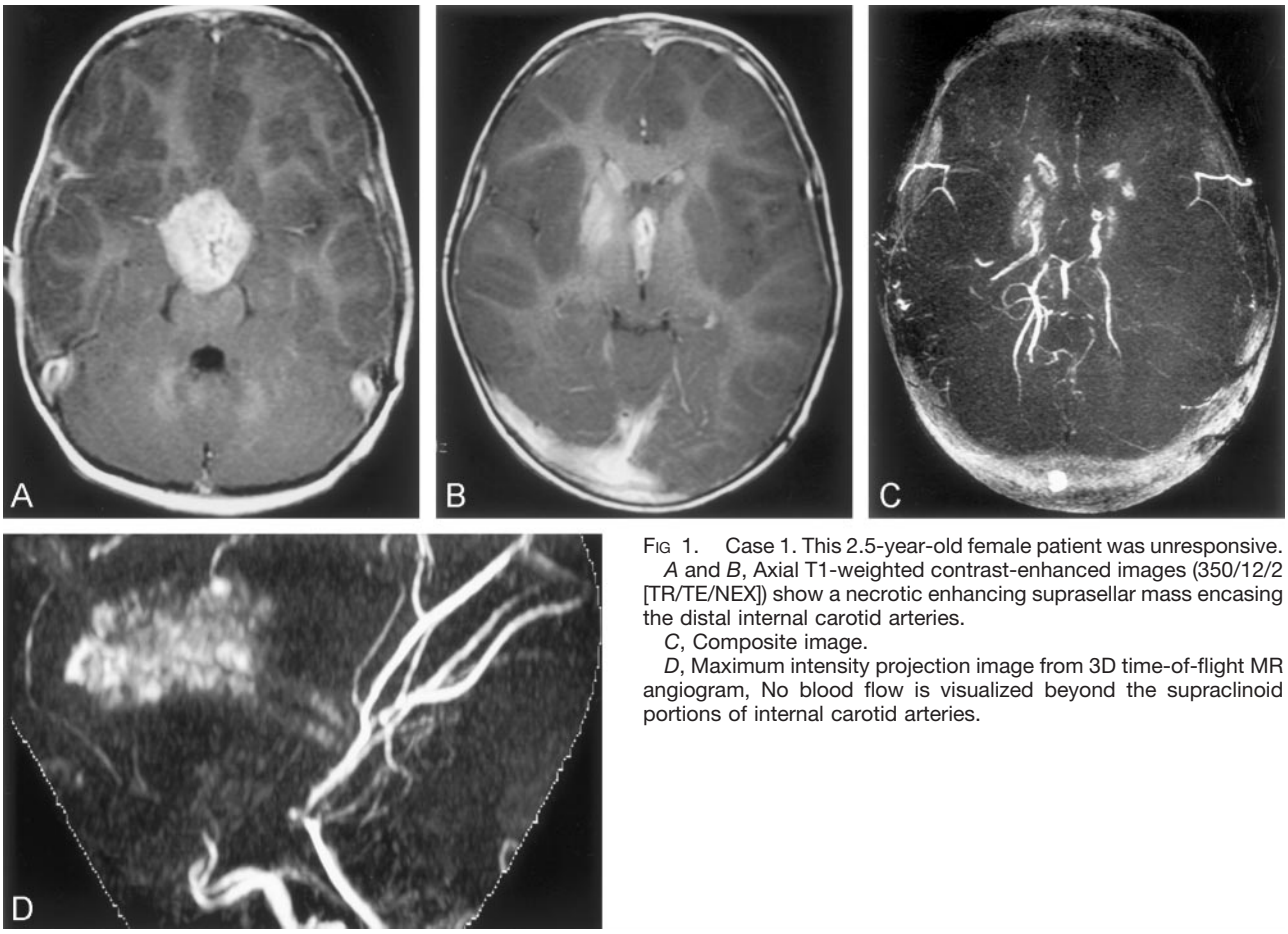

FIG 1. Case 1. This 2.5-year-old female patient was unresponsive.
A and *B*, Axial T1-weighted contrast-enhanced images (350/12/2 [TR/TE/NEX]) show a necrotic enhancing suprasellar mass encasing the distal internal carotid arteries.
C, Composite image.
D, Maximum intensity projection image from 3D time-of-flight MR angiogram, No blood flow is visualized beyond the supraclinoid portions of internal carotid arteries.

on T1- and T2-weighted images because of high cellularity. These tumors also show intense enhancement with contrast material.

Arachnoid cysts may also occur in the suprasellar region. This type of lesion is sharply marginated and is isointense to CSF with all pulse sequences. Unlike the reported cases, arachnoid cysts show no enhancement after contrast administration. Epidermoids are benign tumors that can also be located in the suprasellar region. They are slightly hyperintense relative to CSF with all imaging sequences. Diffusion-weighted images show these lesions to be hyperintense, which serves to distinguish them from arachnoid cysts. Epidermoids also typically do not enhance with contrast material. Dermoid tumors are very heterogeneous in signal intensity. Areas of hyper- and hypointense signal intensity are seen on T1- and T2-weighted images because of the presence of fat and calcification. Similar to arachnoid cysts and epidermoids, this tumor does not enhance after the administration of contrast material.

Light microscopy revealed that all our surgical specimens were composed of a monotonous population of cells with delicate piloid-like processes, loosely arranged within a prominent myxoid background. Focally, the neoplastic cells converged upon small blood vessels in pseudorosette-like formations (Fig 2). Minimal nuclear pleomorphism and few mitotic figures were present. These histomorphologic features are identical to those of a recently described astrocytoma with monomorphous pilomyxoid features (1). The classic pilocytic astrocytoma has characteristic elongated bipolar cells forming loose and compact areas and a variable number of stellate astrocytes in association with Rosenthal fibers and eosinophilic granular bodies.

The newly characterized neoplastic cells lacked these Rosenthal fibers and eosinophilic bodies and the alternating loose and solid areas. These new tumors also lacked the typical hyalinized vessels and papillae of myxopapillary ependymomas (5).

Our surgical specimens showed strong cytoplasmic immunoreactivity with antibodies to glial fibrillary acidic protein and vimentin and nuclear and cytoplasmic staining with S-100 (Fig 3). Glial fibrillary acidic protein, an astrocyte-specific intracellular intermediate filament protein, was also positive on normal tanycyte cells (6). A rare reported case of an intracranial myxopapillary ependymona showed weak staining with glial fibrillary acidic protein and strong staining with vimentin (5). All our cases stained positive for synaptophysin and negative for chromogranin (Fig 3). This is in contrast to astrocytomas and the cases reported by Tihan et al (1), which did not stain for synaptophysin. Synaptophysin is a protein involved in synaptic and synaptoid vesicles and is a marker for any cell with synaptic vesicles. Interestingly, only one of our cases showed dense core gran-

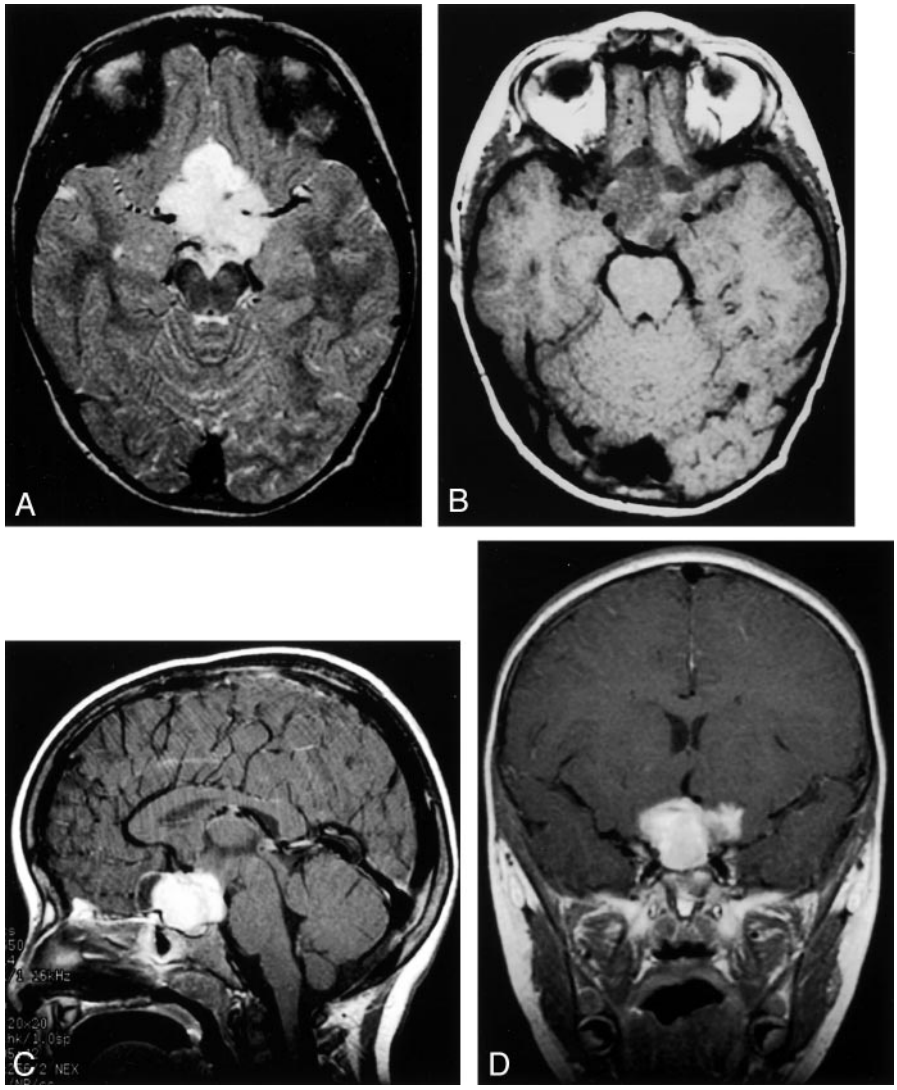

FIG 2. Case 2. Two-year-old male patient with diplopia and a decrease in left eye vision.

A, Axial T2-weighted image (3200/84/1) shows a hyperintense suprasellar mass encasing the anterior portion of the circle of Willis.

B, Axial T1-weighted image (433/16/2) shows a hypointense suprasellar mass encasing the circle of Willis.

C, Contrast-enhanced sagittal T1-weighted image (650/14/2) shows a solid-cystic enhancing hypothalamic-suprasellar mass.

D, Contrast-enhanced coronal view T1-weighted image (400/16/2).

(Continues)

ules when studied ultrastructurally. As speculated by Fuller et al (2), the positivity to synaptophysin may have been due to material bound by the numerous pinocytotic vesicles and coated pits, clear core granules or vesicles of the synaptoid structures, or possibly innate cross-reactivity of the particular synaptophysin antibody used by their laboratory.

Unlike the cases reported by Tihan et al (1), our cases underwent ultrastructural examination. Electron microscopy performed in four cases revealed the presence of neoplastic cell bodies in the third ventricle ependymal lining with long synaptic processes extending to adjacent blood vessels and apical surfaces along with more epithelial-type features of microvilli, cytoplasmic blebs, and rare cilia. Neuronal tumors have true synaptic junctions, whereas this neoplasm displayed synaptoid complexes in closely apposed processes containing vesicles visualized by using electron microscopy (Fig 2). The neoplastic cells in all cases were identical in both staining and electron microscopic characteristics to the normal tanycyte (Fig 2) (2, 3). Tanycytes were described by Horstmann in 1954 (7) and are found in the floor of the fourth ventricle, aqueduct of Sylvius, circumventricular organs, and most commonly in the inferolateral walls of the floor of the third ventricle (6, 7). The tumor cells in our cases shared several common ultrastructural features with the tanycyte, such as microvilli, apical blebs, coated pits, vesicles, intercellular junctions, and singular elongated processes with well-formed end feet (8). Other very rare gliomas, the astroblastoma (9) and subependymoma (10), have had suggested origins from tanycytes. We propose the name *tanycytoma* to describe this new tumor because of its similarity and probable origin from the tanycyte.

Conclusion

The tanycytoma is a newly characterized tumor. The imaging characteristics may not allow for clear differentiation from other intracranial neoplasms, but the hypothalamic-suprasellar location, aggressive nature, and encasement of arteries at the base of the brain should suggest this diagnosis. On the other hand, histologic and electron microscopic findings can confirm the presence of this tumor. The prognosis

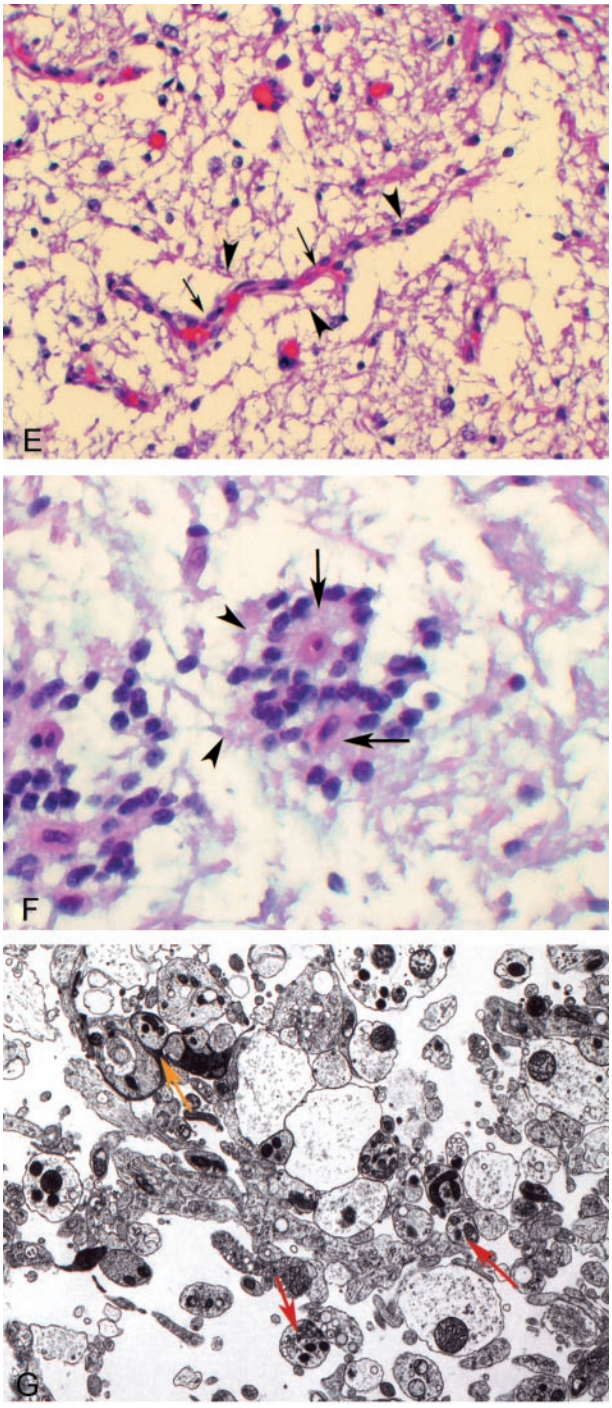

FIG 2. *Continued*

E, Photomicrograph of hematoxylin and eosin-stained normal tanycytes (*arrowheads*) radiating to a blood vessel (*arrows*) in area postrema.

F, Photomicrograph of hematoxylin and eosin-stained neoplastic cells (*arrowheads*) radiating to blood vessel (*arrows*) in tanycytoma specimen.

G, Photomicrograph of electron microscopy of tumor specimen reveals tanycytes with long synaptic processes (*red arrow*) and synaptoid complexes (*yellow arrow*).

for pediatric patients appears worse than for adults, with more aggressive tumors and surgical resection in the hypothalamic-suprasellar region being more difficult. Increased awareness of this neoplasm is required before more definitive statements concerning the diagnosis, treatment, and prognosis of the tanycytoma can be made.

References

1. Tihan T, Fisher PG, Kepner JL, et al. **Pediatric astrocytomas with monomorphous pilomyxoid features and a less favorable outcome.** *J Neuropathol Exp Neurol* 1999;58:1061–1068
2. Fuller CE, Frankel B, Smith M, et al. **Suprasellar monomorphous pilomyxoid neoplasm: an ultrastructural analysis.** *Clin Neuropathol* 2001;6:256–262
3. Millhouse OE, Zellforsch Z, Mikrosk U. *Anat Embryol (Berl)* 1971; 121:1–13
4. Mathew TC, Singh DN. **Morphology and distribution of tanycytes in the third ventricle of the adult rat: a study using semithin methacrylate sections.** *Acta Anat (Basel)* 1989;134:319–321
5. Maruyama R, Koga K, Nakahara T, Kishida K, Nabeshima K. **Cerebral myxopapillary ependymoma.** *Hum Pathol* 1992;23:960–962
6. Flament-Durand J. **Mammalian tanycytes: transmission and scanning electron microscopy.** *Prog Clin Biol Res* 1989;295:363–369
7. Horstmann E. **Die faserglia des Selachiergehirns.** *Z Zellforsch* 1954;39:588–617
8. Flament-Durand J, Brion JP. **Tanycytes: morphology and functions: a review.** *Int Rev Cytol* 1985;96:121–155
9. Rubinstein LJ, Herman MM. **The astroblastoma and its possible cytogenic relationship to the tanycyte: an electron microscopic, immunohistochemical, tissue- and organ-culture study.** *Acta Neuropathol (Berl)* 1989;78:472–483
10. Friede RL, Pollack A. **The cytogenetic basis for classifying ependymonas.** *J Neuropathol Exp Neurol* 1978;37:103–118

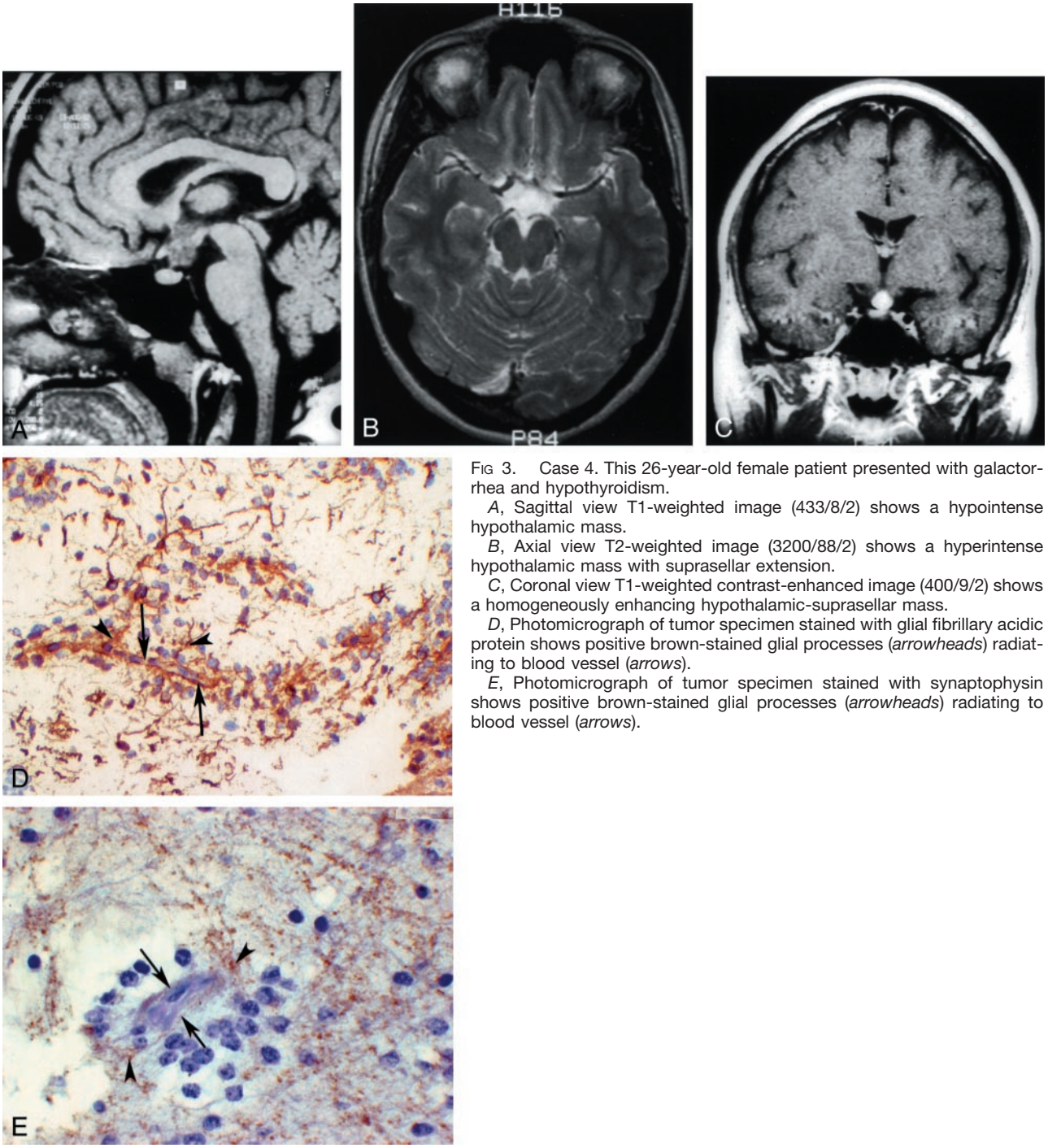

FIG 3. Case 4. This 26-year-old female patient presented with galactorrhea and hypothyroidism.

A, Sagittal view T1-weighted image (433/8/2) shows a hypointense hypothalamic mass.

B, Axial view T2-weighted image (3200/88/2) shows a hyperintense hypothalamic mass with suprasellar extension.

C, Coronal view T1-weighted contrast-enhanced image (400/9/2) shows a homogeneously enhancing hypothalamic-suprasellar mass.

D, Photomicrograph of tumor specimen stained with glial fibrillary acidic protein shows positive brown-stained glial processes (*arrowheads*) radiating to blood vessel (*arrows*).

E, Photomicrograph of tumor specimen stained with synaptophysin shows positive brown-stained glial processes (*arrowheads*) radiating to blood vessel (*arrows*).